INJURY BIOMECHANICS RESEARCH
Proceedings of the Thirty-Eighth International Workshop

Chest Deflection of Relaxed and Braced Human Occupants in Low Severity Frontal Sled Tests and Non-Censored Rib Fracture Data in High Severity PMHS Frontal Sled Tests

A.R. Kemper, S.M. Beeman, and S.M. Duma
Virginia Tech-Wake Forest University, Center for Injury Biomechanics

ABSTRACT

This paper presents the methodologies and results of two studies involving dynamic frontal sled tests. The purpose of the first study was to investigate the effects of pre-impact bracing on the kinematics, kinetics, and chest compression of human volunteers during low-speed frontal sled tests. The purpose of second study was to obtain non-censored rib fracture data and corresponding thoracic injury timing during high severity PMHS frontal sled tests. In the first study, a total of 10 low-speed frontal sled tests (5.0g, Δv=9.7kph) were performed with 5 male human volunteers. Each volunteer was exposed to 2 impulses, one relaxed and the other braced prior to the impulse. In the second study, a total of 3 high severity frontal sled tests (28.6g, Δv=40kph) were performed on two post mortem human surrogates (PMHSs) and one 50th percentile Hybrid III anthropomorphic test device (ATD). A 59 channel chestband, aligned at the nipple line, was used to measure chest deflection for all test subjects in both studies. For PMHS tests, thoracic strain gages allowed for the precise determination of the time of each rib fracture and corresponding AIS injury severity level. In the first study, the chestband data showed that bracing prior to the initiation of the sled pulse essentially eliminated thoracic compression due to belt loading for all human volunteers except one. This study illustrates that muscle activation has a significant effect on the biomechanical response of human occupants in frontal sled tests. In the second study, the sternum compression data and maximum chest compression data, which did not occur at the sternum, illustrated that serious thoracic injury (AIS=3) occurs before peak compression and at lower chest compressions than the current ATD thoracic injury criterion. In addition, the chestband data showed that maximum chest compression had a more reasonable correlation between compression and injury timing than sternum compression. Therefore, an ATD with multiple chest deflection measurement locations would be advantageous. Overall, the two studies provide critical data that can be used in the design and validation of advanced ATDs and finite element models, as well as the establishment of improved, more stringent thoracic injury criteria.

INTRODUCTION

In the United States, approximately 27,000 vehicle occupant fatalities occur annually, with frontal collisions accounting for approximately 50% of these fatalities (NHTSA Traffic Safety Facts, 2008). In addition, the number of occupants sustaining injuries greatly exceeds the number of fatalities. Injuries sustained in motor vehicle collisions range from non-life threatening eye and upper extremity injuries to more serious head and chest injuries (Duma et al., 2000; Duma et al., 2003; Kennedy et al., 2004; Jernigan et al., 2005; Kemper et al., 2008; Cormier and Duma, 2009; Gayzik et al., 2009; Kemper et al., 2009; Duma et al. 2011; Kemper et

al., 2011). For belted drivers in frontal collisions, the chest is the body region which most frequently sustains a serious injury (AIS≥ 3) (Brumbelow and Zuby, 2009). For side impact collisions, it has been reported that thoracic injuries are the most common type of serious injury (AIS≥3) to vehicle occupants in both near side and far side crashes which do not involve a rollover (Samaha et al., 2003; Gabler et al., 2005).

Computational models and anthropomorphic test devices (ATDs) are commonly used to predict and evaluate human occupant responses and injuries in motor vehicle collisions. These tools have proved invaluable in the mitigation of thoracic injuries and reduction of fatalities. However, they are primarily validated against post mortem human surrogate (PMHS) data, which does not include the effects of muscle activation. Although studies have shown that tensing muscles prior to a collision event can change occupant kinetics and kinematics during the collision, no studies have quantified the chest compression experienced by volunteers during a dynamic sled test (Armstrong et al., 1968; Hendler et al., 1974; Begeman 1980; Sugiyama 2007; Ejima 2008). In addition, the literature regarding thoracic loading in full scale PMHS experiments has been predominately focused on developing global criteria for predicting thoracic injury (Eppinger, 1976; Morgan et al., 1986; Viano, 1989; Morgan et al., 1994; Pintar et al., 1997; Kuppa and Eppinger, 1998; Kuppa et al., 2003). These include force, acceleration, and displacement based criteria, as well as combinations of these engineering parameters. Although the thoracic injury criteria reported in these studies provide biomechanically-based metrics for injury risk, they are limited by the fact that they were developed based on the results of PMHS studies which relied primarily on censored rib fracture data. In other words, only the total number of rib fractures resulting from a given impact is known. Therefore, the force and thoracic deflection corresponding to the injury timing could not be determined. Consequently, these studies rely on statistical models to develop injury risk functions with respect to global criteria, such as peak chest deflection or peak acceleration. However, many cadaveric studies on other body parts have shown that fractures occur before peak force and deflection (Duma et al., 1999; Duma et al., 2003a; Duma et al., 2003b; Cormier et al., 2011).

To address the limitations in the literature, this paper presents the methodologies and results of two studies involving dynamic frontal sled tests. The purpose of the first study was to investigate the effects of pre-impact bracing on the kinematics, kinetics, and chest compression of human volunteers during low-speed frontal sled tests. The purpose of second study was to obtain non-censored rib fracture data and corresponding thoracic injury timing during high severity PMHS frontal sled tests.

METHODS

Volunteer Testing

A total of 10 low-speed frontal sled tests (5.0g, Δv=9.7kph) were performed with 5 male human volunteers (Table 1). Selected volunteers were approximately 50th percentile male height and weight (175cm; 76.7kg) (Schneider et al., 1983). Approval to conduct the human subject testing presented in the current study was granted by the Virginia Tech Internal Review Board (IRB). In addition, all volunteers signed an informed consent form prior to participating in the study.

Table 1: Volunteer subject information.

Measurement	Units	Subject ID Number				
		S1	S2	S3	S4	S5
Age	(yr)	19	23	20	19	20
Gender	(M/F)	Male	Male	Male	Male	Male
Weight	(kg)	72.8	78.0	81.6	73.6	76.8
Height	(cm)	174.0	171.8	175.3	176.5	176.4

Experimental Setup

Dynamic frontal sled tests were performed using a custom mini-sled and test buck (Figure 1). The mini-sled was accelerated with a pneumatic piston, which was used to generate a frontal sled pulse (5.0g, Δv=9.7kph) (Figure 2). The consistency in the sled acceleration between subjects for a given test condition shows that the custom mini-sled was extremely repeatable. The maximum sled pulse severity was determined based on previous research which has shown that a frontal sled pulse of this severity does not result in injury (Arbogast et al., 2009).

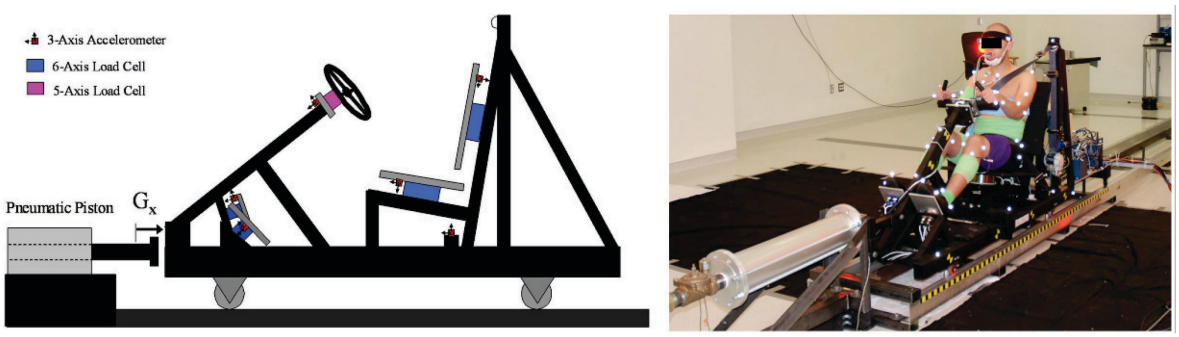

Figure 1: Test buck schematic (left) and subject seated on test buck (right).

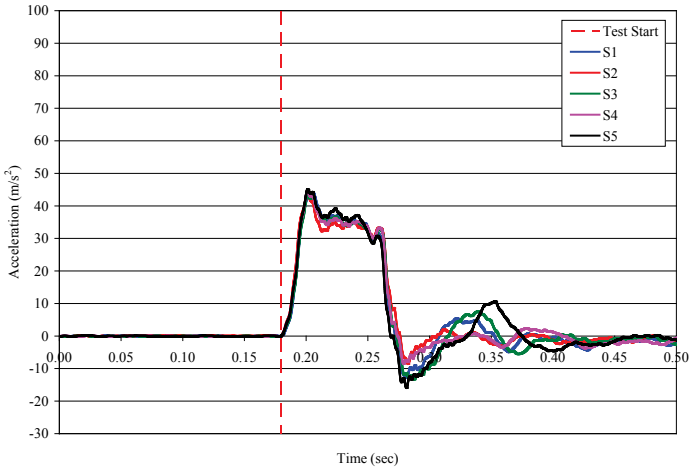

Figure 2: Sled acceleration pulse (x-direction) used for volunteers.

The test buck was instrumented with 5 multi-axis load cells and 18 single-axis accelerometers. A six-axis load cell was installed on both the seatpan and seatback (Robert A. Denton, Inc., 44 kN-Model 2513, Rochester Hills, MI). A six-axis load cell was installed on the right foot support (Robert A. Denton, Inc., 13.3 kN-Model 1794A, Rochester Hills, MI) and left foot support (Robert A. Denton, Inc., 13.3 kN-Model 1716A, Rochester Hills, MI). A five-axis load cell was installed on the steering column (Robert A. Denton, Inc., 22.2 kN-Model 1968, Rochester Hills, MI). Three-axis accelerometer cubes (Endevco 7264B, 2000 g, San Juan Capistrano, CA) were rigidly mounted to each load cell plate for inertial compensation. The test buck acceleration was measured with a three-axis accelerometer cube (Endevco 7264B, 2000 g, San Juan Capistrano, CA) rigidly mounted to the frame under the seatpan. Seatbelt tension load sensors were added to the retractor, shoulder, and lap portions of the seatbelt (Robert A. Denton, Inc., 13.3 kN-Model 3255, Rochester Hills, MI). Seatbelt spool out at the retractor was measured with a potentiometer (Space Age Control Inc. 160-1705, 539.75mm, Palmdale, CA) attached to a custom seatbelt clamp.

Subject Instrumentation

A 59 channel chestband (Denton, Inc., Model 8641, Rochester Hills, MI) was used to quantify thoracic displacement and chest contours throughout the duration of the trials (Eppinger, 1989; Yoganandan et al., 1991; Kallieris et al., 1995; Shaw et al, 2006; Forman et al., 2006). Gage 1 was positioned at the spine and the band was wrapped around the chest, aligned with the nipple line, so that gage number ascended in the clockwise direction (Figure 3). Heavy duty double sided adhesive tape was used to securely attach the chestband to each subject. The chestband was then wrapped with co-flex, a self-adherent compression wrap, to ensure a tight connection and protect the chestband wires throughout each trial.

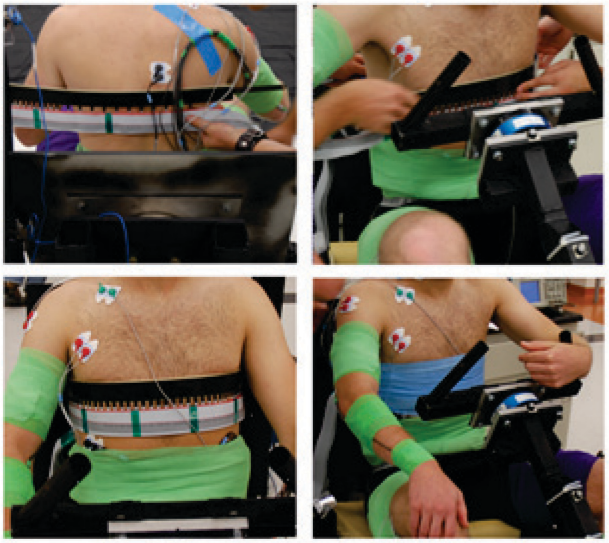

Figure 3: Chestband aligned with the nipple line of the chest.

In addition to the chestband data, a number of other subject measurements were recorded during each trial. For each subject, accelerations were measured at the sternum, spine, and head. Surface electromyography (EMG) was obtained from a total of 20 muscles (right/left thigh, right/left shank, right arm, abdomen, back, and neck) during each test event. However, since the focus of the current study is kinetics and chest compression, the results of subject acceleration and EMG data are not presented.

Test Conditions

Each volunteer was exposed to two 5.0 g (Δv=9.7kph) frontal sled impulses, one relaxed and the other braced prior to the impulse. For all tests, a load limiting driver side seatbelt was placed around the test subject, and the slack was removed. Volunteers were informed before each test as to whether they were to remain relaxed or brace themselves for the sled impulse. For the relaxed tests, a television monitor was used as a distraction mechanism and the trigger was out of sight so that the volunteers were unaware of when the test would occur. Prior to the relaxed tests, subjects were instructed to relax and continue to watch the monitor while facing forward. The sled pulse was then randomly initiated after several minutes of quiet sitting. For the braced tests, subjects were asked to brace themselves with both their arms and legs. A guided countdown was used to instruct the volunteers when to brace prior to the initiation of the sled pulse. Each subject had a waiting time of approximately 30 minutes between subsequent tests.

Data Acquisition and Processing

An onboard data acquisition system was used to record 148 channels of data at a sampling rate of 20kHz. For relaxed tests, data was collected during the relaxed state and test event. For braced tests, data was collected during the relaxed state, braced state, and test event. All load cells were zeroed without the subject seated on the test buck. All reaction load cell data were compensated for crosstalk and then inertially compensated, with the use of three single-axis accelerometers mounted to each reaction plate. The reaction load cell data and test buck accelerometer data were filtered using SAE Channel Frequency Class (CFC) 60 (SAE J211, 1995). The seatbelt load cell data were filtered using CFC 180. The unfiltered chestband data

were processed using RBand-PC software, to generate two-dimensional chest contours in 10ms increments as well as the deflection between the spine and sternum (Kallieris et al., 1995; Shaw et al, 2006). Chest compression was defined as the ratio of the instantaneous chest depth to the chest depth measured 10 ms prior to the incitation of the sled pulse.

A Vicon motion analysis system, consisting of 12 MX-T20 2 megapixel cameras, was used to quantify the three-dimensional kinematics (±1mm) of photo-reflective markers placed on both the test subject and the test buck at a sampling rate of 1kHz (Figure 4). Marker trajectories were converted to the reference frame of the test buck and then to the SAE J211 sign convention (SAE J211, 1995). The excursions of specified regions of interest were normalized to their respective initial positions and compared by test condition across subjects. In addition, high-speed video was obtained from the lateral aspect of the volunteer at a sampling rate of 1kHz with the use of a high resolution camera (Vision Research, Phantom V9, Wayne, NJ).

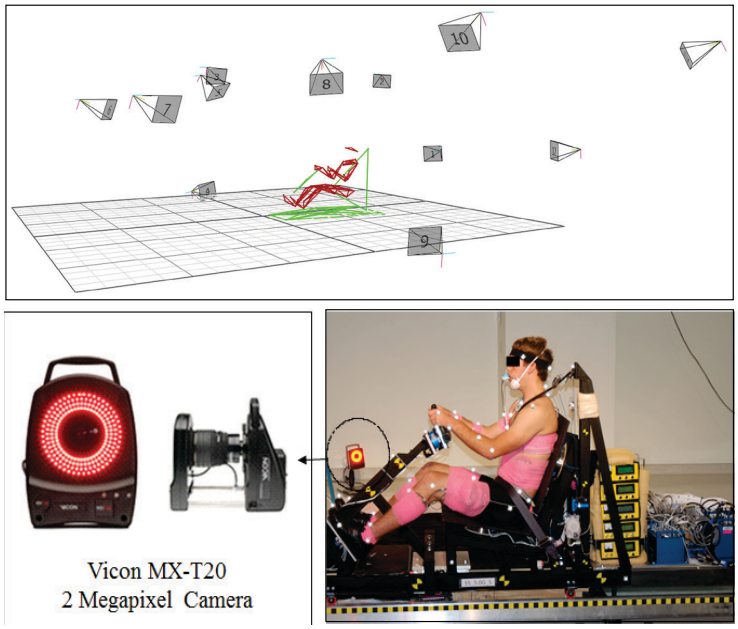

Figure 4: Vicon System and markers.

After completing the trials and approximately one week after the trials were performed, each subject was asked if they experienced any pain or discomfort as a result of the experiments. One subject reported mild discomfort to his lower back as a result of contacting the seatback during the 5g relaxed trial. None of the other subjects reported any pain or discomfort as a result of the experiments.

PMHS Testing

A total of 3 high severity frontal sled tests were performed on two PMHS and one 50th percentile Hybrid III ATD (Table 2). Selected PMHSs were close to the 50th percentile male height and weight (175cm; 76.7kg) (Schneider et al., 1983).

Table 2: PMHS information.

Measurement	Units	Subject ID	
		PMHS 1	PMHS 2
Age	(yr)	63	79
Gender	(M/F)	Male	Male
Weight	(kg)	68.6	86.4
Height	(cm)	176.0	184.0

Experimental Setup

The PMHS sled tests were performed using a 1.4 MN ServoSled system manufactured by Seattle Safety (Figure 5). The high severity sled pulse was designed to match the vehicle acceleration of a popular 2007 sedan obtained during one of the FMVSS 208 standard crash tests (28.6g, Δv=40kph) (Figure 6). The sled pulse started at t=180ms for all tests.

For all tests, a load limiting (5kN) driver side seatbelt was placed around the test subject, and the slack was removed. It should be noted that the pretensioner was not activated for any of the tests. The lungs were pressurized prior to each test with the use of a tracheostomy tube. The arterial vessels were pressurized prior to each test with the use of a tube inserted in the left carotid artery. The head, legs, and hands were held in place with the use of masking tape attached to the test buck. Prior to testing, the masking tape on the legs, hands, and head was cut slightly to ensure that it would tear free during the test.

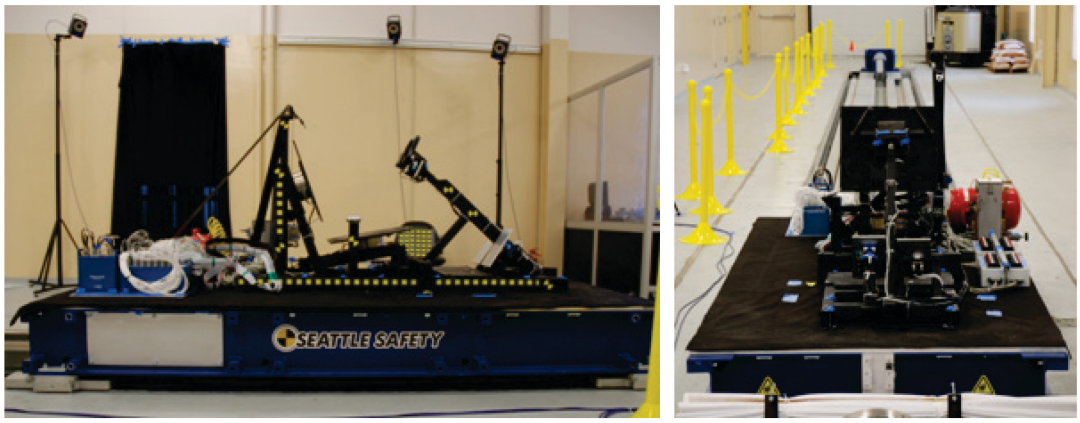

Figure 5: Test buck mounted on ServoSled.

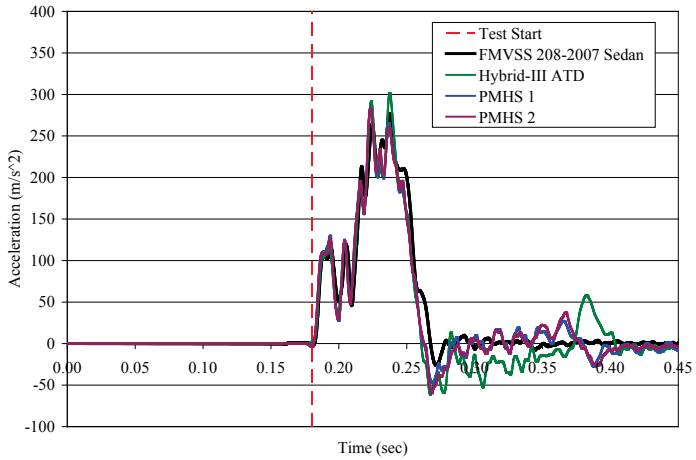

Figure 6: High severity sled acceleration pulse (x-direction) used for PMHS tests.

The test buck used for the PMHS tests was the exact test buck used for the volunteer testing (Figure 1). The test buck was instrumented with 5 multi-axis load cells and 18 single-axis accelerometers. A six-axis load cell was installed on both the seatpan and seatback (Robert A. Denton, Inc., 44 kN-Model 2513, Rochester Hills, MI). A six-axis load cell was installed on the right foot support (Robert A. Denton, Inc., 13.3 kN-Model 1794A, Rochester Hills, MI) and left foot support (Robert A. Denton, Inc., 13.3 kN-Model 1716A, Rochester Hills, MI). A five-axis load cell was installed on the steering column (Robert A. Denton, Inc., 22.2 kN-Model 1968, Rochester Hills, MI). Three-axis accelerometer cubes (Endevco 7264B, 2000 g, San Juan Capistrano, CA) were rigidly mounted to each load cell plate for inertial compensation. The test buck

acceleration was measured with a three-axis accelerometer cube (Endevco 7264B, 2000 g, San Juan Capistrano, CA) rigidly mounted to the frame under the seatpan. Seatbelt load sensors were added to the shoulder belt and lap belt (Robert A. Denton, Inc., 13.3 kN-Model 3255, Rochester Hills, MI). Seatbelt spool out at the retractor was measured with a potentiometer (Space Age Control Inc. 160-1705, 539.75mm, Palmdale, CA) attached to a custom seatbelt clamp.

Subject Instrumentation

A total of 23 single-axis strain gages (Vishay Micro-Measurement, CEA-06-062UW-350, Shelton, CT) were attached to the thorax of the PMHS (Figure 7). One strain gage was attached to the sternum. One strain gage was attached to the left clavicle at the midpoint. Thirteen strain gages were attached to the right side of the rib cage (lateral region of ribs 3-7 and anterior region of ribs 2-9). Eight strain gages were attached to the left side of the rib cage (anterior region of ribs 2-9).

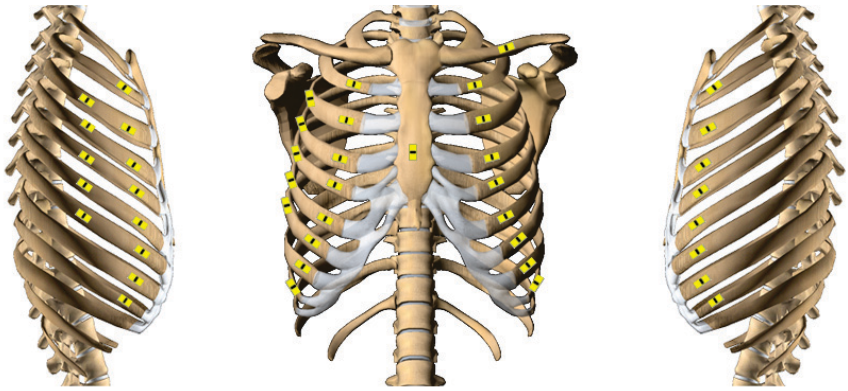

Right View Anterior View Left View

Figure 7: Thoracic strain gage locations.

Once the location of each strain gage was determined, the soft tissue and periosteum were removed and the bone was swabbed with ether to locally dry the bone. Upon drying, an acidic solution (Vishay Micro-Measurement, Conditioner A, Shelton, CT) was applied to the surface with a clean piece of gauze to etch the surface of the bone. Then, a basic solution (Vishay Micro-Measurement, Neutralizer 5A, Shelton, CT) was applied to the surface to neutralize the acidic solution. The gage was removed from its case and prepared for mounting by applying a catalyst (Vishay Micro-Measurement, M-Bond 200 Catalyst, Shelton, CT) to the underside of the gage. Next, an adhesive (Vishay Micro-Measurement, M-Bond 200 Adhesive, Shelton, CT) was applied to the bone and the gage was quickly pushed over the adhesive in a rolling manner. The strain gage was covered with a small piece of latex and held with firm pressure for 3 minutes. Special care was taken to align each gage so that it was in line with the axis of the rib. Finally, the strain gage wire was strain relieved with a zip tie placed around the rib.

A 59 channel chestband (Denton, Inc., Model 8641, Rochester Hills, MI) was used to quantify thoracic displacement and chest contours throughout the duration of the trials (Eppinger, 1989; Yoganandan et al., 1991; Kallieris et al., 1995; Shaw et al, 2006; Forman et al., 2006). Gage 1 was positioned at the spine and the band was wrapped around the chest, aligned with the nipple line, so that gage number ascended in the clockwise direction (Figure 8). Heavy duty double sided adhesive tape was used to secure the end of the chestband to the chestband itself. The chestband was securely attached to the PMHS with sutures placed through the skin and around the chestband. The chestband was then wrapped with co-flex, a self-adherent compression wrap, to ensure a tight connection and protect the chestband wires throughout each trial.

In addition to the strain gage and chestband data, a number of other measurements were recorded during each PMHS trial. For each subject, three-axis accelerometer cubes were rigidly mounted to the head, sternum, C7, T7, T12, sacrum, left/right femur, and left/right tibia. Angular velocity of the head was also measured. However, since the focus of the current study is chest compression, the results of subject acceleration are not presented.

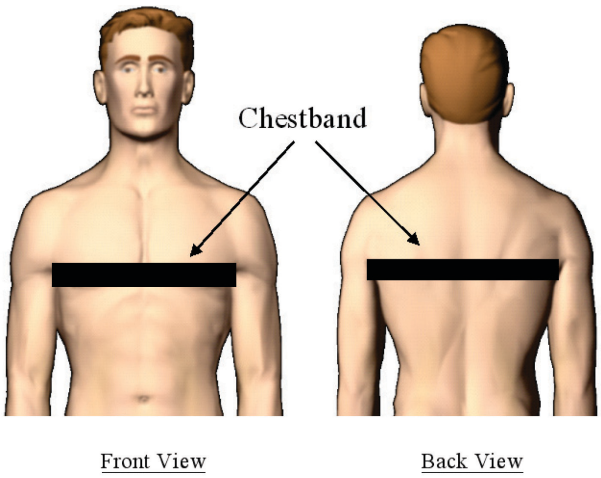

Figure 8: Chestband aligned with the nipple line of the chest.

Data Acquisition and Processing

An onboard data acquisition system was used to record 172 channels of data at a sampling rate of 20kHz. All load cells were zeroed without the subject seated on the test buck. All reaction load cell data were compensated for crosstalk and then inertially compensated, with the use of three single-axis accelerometers mounted to each reaction plate. The reaction load cell data and test buck accelerometer data were filtered using SAE Channel Frequency Class (CFC) 60 (SAE J211, 1995). The seatbelt load cell data were filtered using CFC 180. The strain gage data was not filtered. The unfiltered chestband data were processed using RBand-PC software, to generate two-dimensional chest contours in 10ms increments as well as the deflection between the spine and sternum. Chest compression was defined as the ratio of the instantaneous chest depth to the chest depth measured 10 ms prior to the incitation of the sled pulse.

A Vicon motion analysis system, consisting of 12 MX-T20 2 megapixel cameras, was used to quantify the three-dimensional kinematics (±1mm) of photo-reflective markers placed on both the test subject and the test buck at a sampling rate of 1kHz (Figure 9). Marker trajectories were converted to the reference frame of the test buck and then to the SAE J211 sign convention (SAE J211, 1995). The excursions of specified regions of interest were normalized to their respective initial positions and compared by test condition across subjects. In addition, high-speed video was obtained from the lateral aspect of the volunteer at a sampling rate of 1kHz with the use of a high resolution camera (Vision Research, Phantom V9, Wayne, NJ).

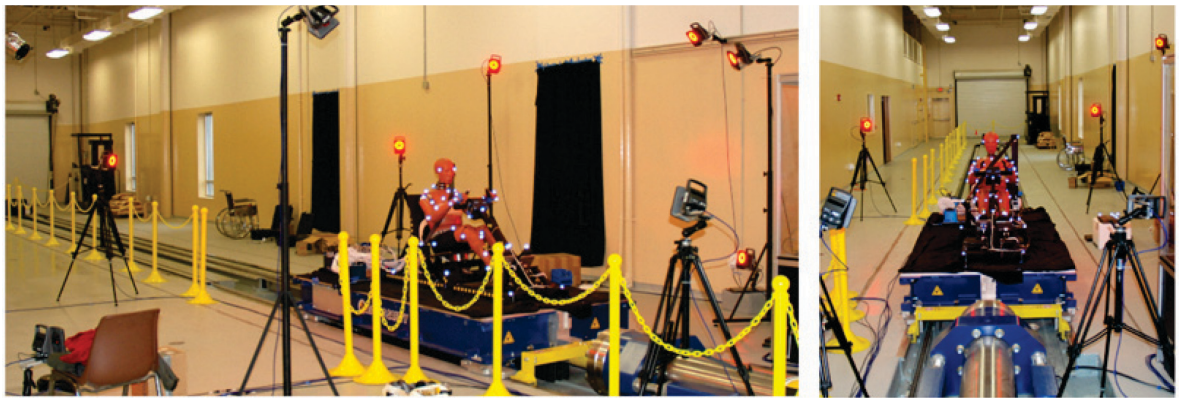

Figure 9: Vicon System and markers on Servo Sled.

RESULTS

Volunteer Testing

Qualitative examination of the global trajectories of each test subject revealed marked differences between the relaxed and braced conditions in both initial position and forward excursions of the volunteer occupants (Figure 10). The normalized data highlighted pronounced differences in forward excursions due to bracing. It was found that bracing significantly reduced the forward excursion of the elbows ($p<0.01$), shoulders ($p<0.01$), and head ($p<0.01$). Although not significant, bracing considerably reduced the forward excursion of the lower extremities and pelvis.

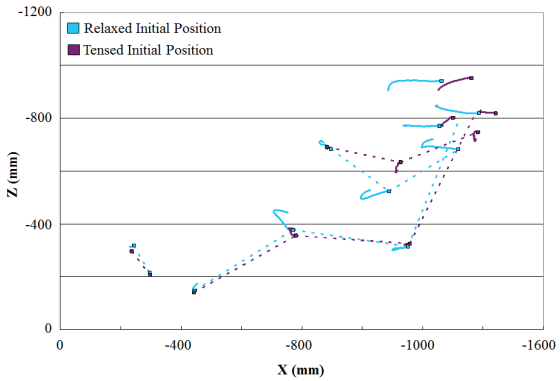

Figure 10: Example global trajectory of a relaxed vs. braced volunteer test.

Example 2D chestband contours were plotted for each test condition (Figure 11). In each figure, the red line represents the subject's chest contour 10 ms before the start of the trial and the blue line represents the subject's chest contour at the time of peak sternum deflection. For the braced trial, the red line represents the subject's chest contour while in a braced state, while the green line represents the subject's chest contour prior to bracing, i.e. relaxed state.

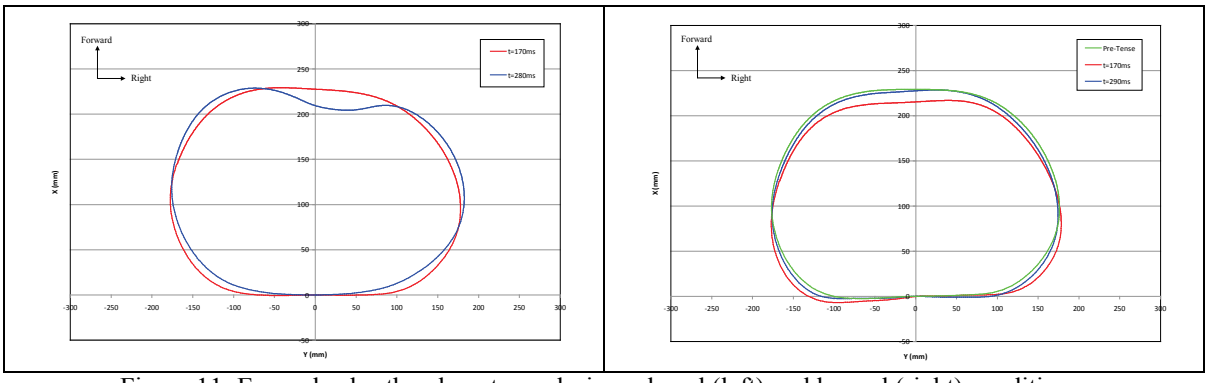

Figure 11: Example chestband contours during relaxed (left) and braced (right) conditions.

The chest compression for each subject was plotted for each test condition (Figure 12). Chest compression was defined as the ratio of the instantaneous chest depth at the sternum to the chest depth at the sternum measured 10 ms prior to the incitation of the sled pulse. It should be noted that for the braced condition, the volunteers were in a braced state 10 ms prior to the initiation of the sled pulse. Positive chest compression indicates a decrease in chest depth at the sternum, while negative chest compression indicates an increase in chest depth at the sternum.

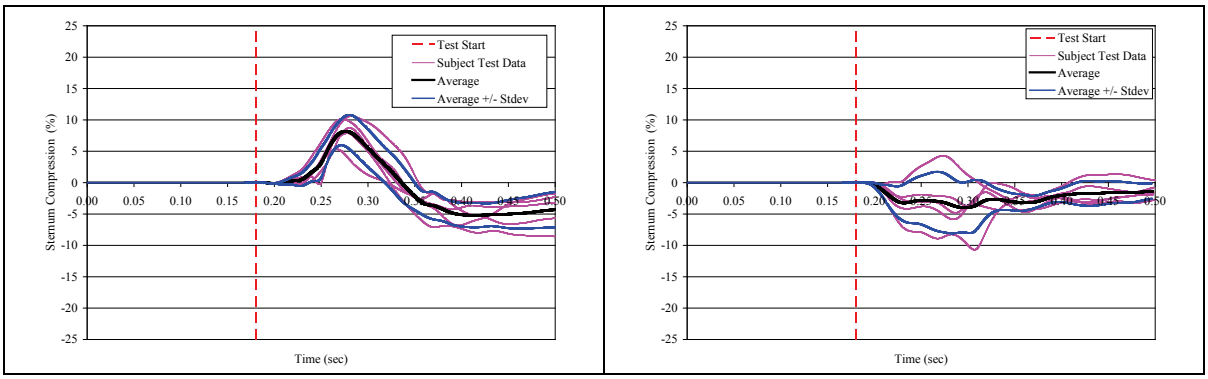

Figure 12: Sternum compression during relaxed (left) and braced (right) conditions.

PMHS Testing

The global trajectories of the selected markers, in the sagittal plane, were plotted up to the point of maximum forward head excursion for each test severity (Figure 13). The subject's initial posture in sagittal plane was illustrated in the global coordinates using connecting lines.

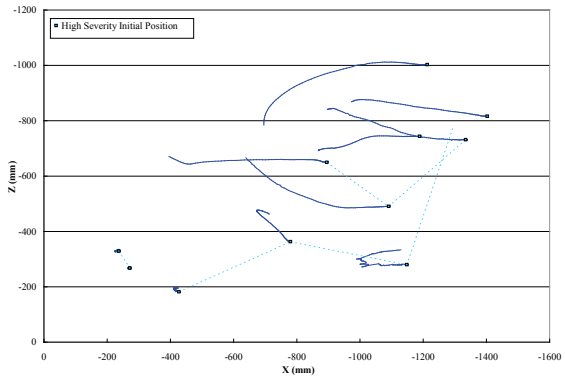

Figure 13: PMHS 1 global trajectory of selected markers.

The injury analysis for each subject was conducted by means of gross dissection preformed by a certified medical doctor. The documented chest injuries for PMHS 1 and 2 are summarized in Figure 14. The gross dissection of the thorax of PMHS 1 revealed a total of fifteen (n=15) rib fractures. The gross dissection of the thorax of PMHS 2 revealed a total of twenty six (n=26) rib fractures.

PMHS 1	PMHS 2
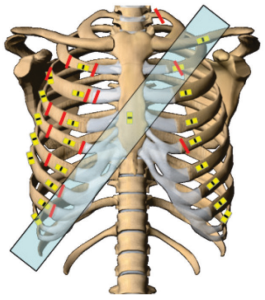 **AIS = 3** 12 Right Side Fractures 3 Left Side Fractures	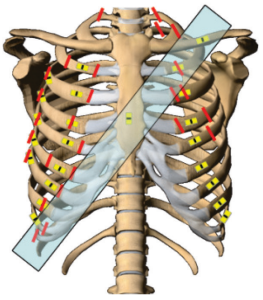 **AIS = 4** 17 Right Side Fractures 9 Left Side Fractures

Figure 14: Chest injury summary for PMHS 1 and 2.

The time histories of each strain gage were analyzed to determine the time at which each rib fracture occurred. The timing of the fractures is indicated by an extremely sharp drop in rib strain (Figure 15). Fractures that occur directly under strain gages are of particular interest because the true failure strain at the time of fracture can be obtained.

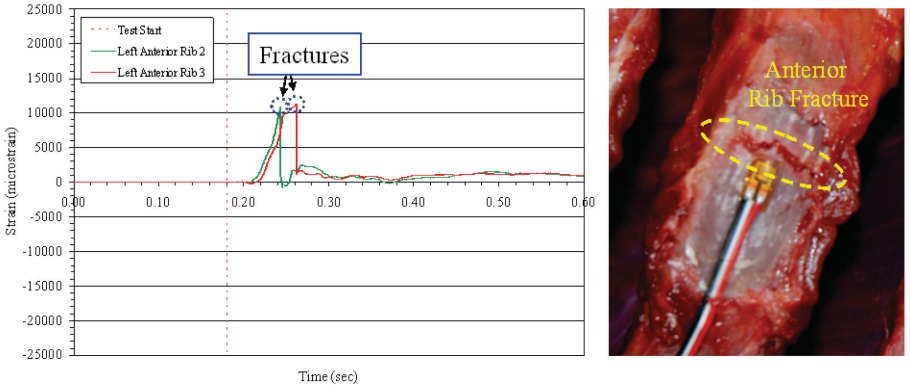

Figure 15: Determination of rib fracture timing.

The two dimensional chestband contours for each subject were plotted for the ATD and each PMHS (Figures 16 and 17). The red line represents the subject's chest contour 10 ms before the start of the sled pulse. The blue line represents the subject's chest contour at the time of peak sternum deflection. For all subjects, the maximum chest compression occurred to the right of the sternum.

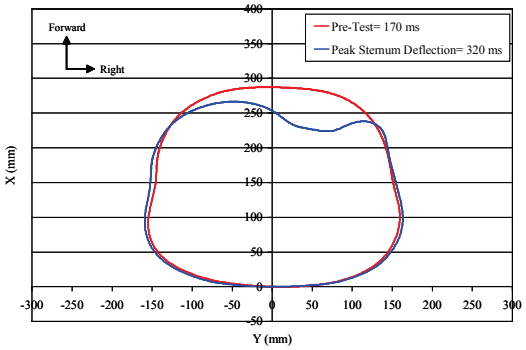

Figure 16: Chestband contours for Hybrid III ATD.

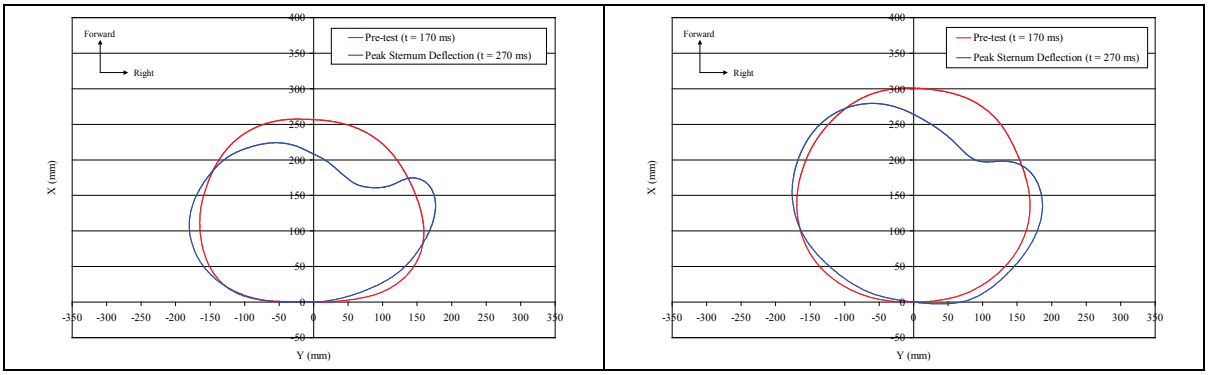

Figure 17: Chestband contours for PMHS 1 (left) and PMHS 2 (right).

The internal and external sternum deflections measured for the Hybrid III ATD are shown in Figure 18. The sternum deflections for the ATD were found to be well below the current thoracic injury criteria. However, both PMHSs sustained AIS 3+ thoracic injuries. The sternum compression for PMHS 1 and PMHS 2 were

plotted along with the rib fracture timing and AIS injury timing (Figure 19). The results show that for both PMHSs, AIS=3 occurred both before peak compression and at a considerably lower sternum compression than the current criterion.

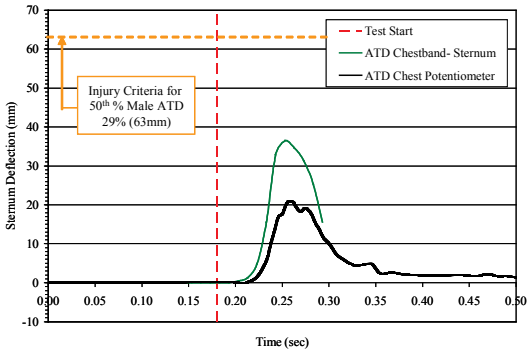

Figure 18: Sternum deflections for Hybrid III ATD.

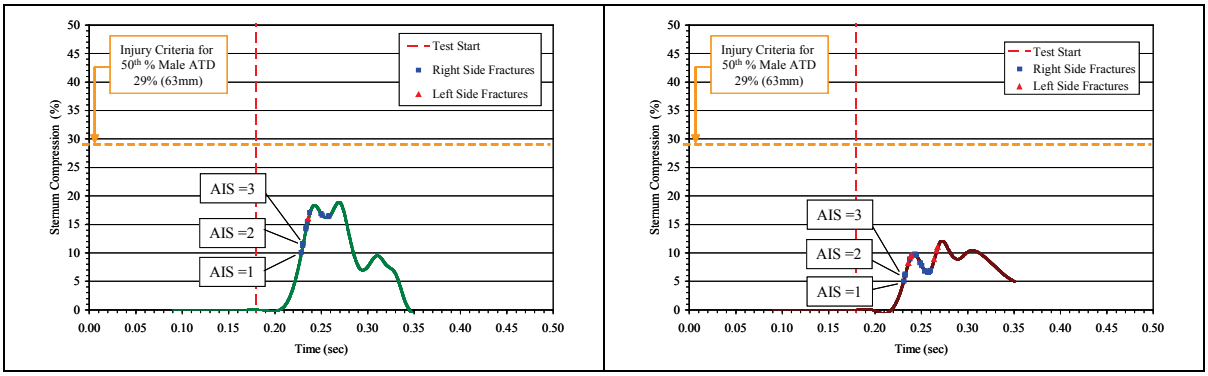

Figure 19: Sternum compression, fracture timing, and injury timing for PMHS 1 (left) and PMHS 2 (right).

As illustrated in Figures 16 and 17, the maximum chest compression did not occur at the sternum for the ATD or PMHSs. Therefore, the maximum chest compression for PMHS 1 and PMHS 2 were plotted along with the rib fracture timing and AIS injury timing (Figure 20). A clear inflection point can be seen after the first few rib fractures occurred, indicating structural compromising of the rib cage. The maximum chest compression results show a more reasonable correlation between compression, rib fracture timing, and injury than sternum compression. However, results show that AIS=3 occurred both before peak compression and at a lower chest compression than the current thoracic criterion for both PMHSs even when using maximum chest compression.

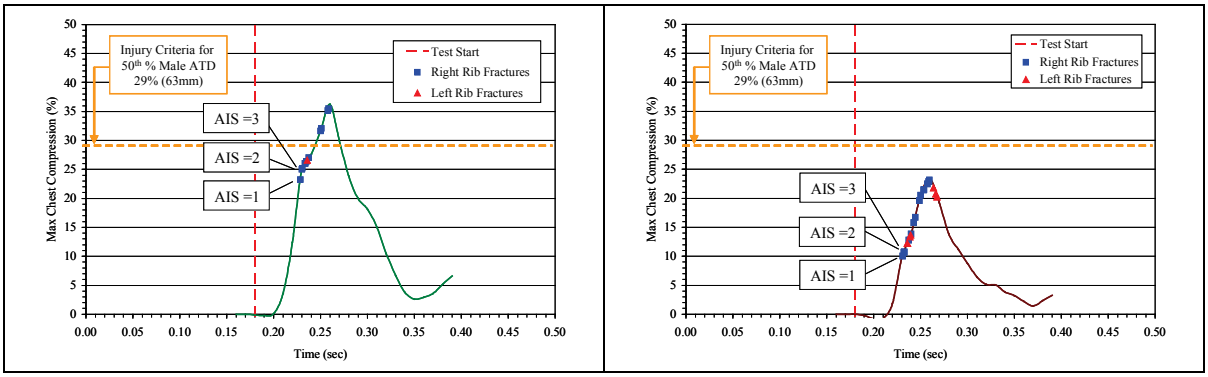

Figure 20: Maximum compression, fracture timing, and injury timing for PMHS 1 (left) and PMHS 2 (right).

CONCLUSIONS

Volunteer Testing

A total of 10 low-speed frontal sled tests (5.0g, Δv=9.7kph) were performed with 5 male human volunteers. The height and weight of the human volunteers were approximately that of the 50th percentile male. Each volunteer was exposed to 2 impulses, one relaxed and the other braced prior to the impulse. A 59 channel chestband, aligned at the nipple line, was used to measure anterior-posterior sternum deflection for all test subjects. The chestband data showed that bracing prior to the initiation of the sled pulse eliminated thoracic compression due to belt loading for all subjects except one. The load cell data indicate that forces were distributed through the feet, seatpan, and steering column as opposed to the seatbelt for the bracing condition. In addition, the forward excursion of the elbows and shoulders were significantly reduced during the braced condition compared to the relaxed condition. The data from the volunteer testing illustrates that muscle activation has a significant effect on the biomechanical response of human occupants in frontal impacts and can be used to refine and validate computational models and ATDs used to assess injury risk in automotive collisions.

PMHS Testing

A total of 3 high severity frontal sled tests were performed on two post mortem human surrogates and one 50th percentile Hybrid III ATD. A 59 channel chestband, aligned at the nipple line, was used to measure anterior-posterior sternum deflection and maximum deflection for all test subjects. For PMHS tests, thoracic strain gages allowed for the precise determination of the time of each rib fracture and corresponding AIS injury severity level. Although the internal and external sternum deflections measured for the Hybrid III ATD were found to be well below the current thoracic injury criterion, both PMHSs sustained AIS 3+ thoracic injuries. The sternum compression data and maximum chest compression data, which did not occur at the sternum, illustrated that serious thoracic injury (AIS=3) occurs before peak compression and at lower chest compressions than the current ATD thoracic injury criterion. In addition, the chestband data showed that maximum chest compression had a more reasonable correlation between compression and injury timing than sternum compression. Therefore, an ATD with multiple chest deflection measurement locations would be advantageous. Overall, this study provides critical data that can be used in the design and validation of advanced ATDs and finite element models, as well as the establishment of improved, more stringent thoracic injury criteria.

ACKNOWLEDGEMENTS

The authors would like to thank Toyota Motor Engineering & Manufacturing (TEMA) and Toyota Central Research and Development Laboratories (TCRDL) for sponsoring this research.

REFERENCES

ARBOGAST, K.B., BALASUBRAMANIAN, S., SEACRIST, T., MALTESE, M.R., GARCÍA-ESPAÑA, J.F., HOPELY, T., CONSTANS, E., LOPEZ-VALDES, F.J., KENT, R.W., TANJI, H., AND HIGUCHI, K., Comparison of kinematic responses of the head and spine for children and adults in low-speed frontal sled tests. Stapp Car Crash J., 53, 329-372, 2009.

ARMSTRONG, R.W., WATERS, H.P, AND STAPP, J.P., Human muscular restraint during sled deceleration. Stapp Car Crash J., 12, 440-462, 1968.

BEGEMAN, P. C., KING, A.I., LEVINE, R.S., VIANO, D.C., Biodynamic response of the musculoskeletal system to impact acceleration. SAE Paper 801312, 479-509, 1980.

BRUMBELOW, M.L, AND ZUBY, D.S. Impact and injury patterns in frontal crashes of vehicles with good ratings for frontal crash protection. Proceedings of the 21st International Technical Conference on the Enhanced Safety of Vehicles, Paper Number 09-0257, 2009.

CORMIER, J.M. AND DUMA, S.M., Epidemiology of facial fractures in automotive collisions, Annals of Advances in Automotive Medicine. 63, 169-176, 2009.

CORMIER, J., MANOOGIAN, S., BISPLINGHOFF, J., ROWSON, S., SANTAGO, A., MCNALLY, C., DUMA, S.M., BOLTE, J., The tolerance of the frontal bone to blunt impact. *Journal of Biomechanical Engineering.* 133(2): 021004, 2011.

DUMA, S.M., SCHREIBER, P.H., MCMASTER, J.D., CRANDALL, J.R., BASS, C.R., AND PILKEY, W.D., Dynamic Injury Tolerance for Long Bones in the Female Upper Extremity. *Journal of Anatomy*. 194(3): 463-71, 1999.

DUMA, S.M. AND CRANDALL, J.R., Eye injuries from airbags with seamless module covers. J Trauma. 48, 786-9, 2000.

DUMA, S.M., BOGGESS, B.M, CRANDALL, J.R., AND MACMAHON,C.B., Injury risk function for the small female wrist in axial loading. *Accident Analysis and Prevention*. 35(6): 869-875, 2003a.

DUMA, S.M., BOGGESS, B.M., CRANDALL, J.R., HURWITZ, S.R., SEKI, K. AND AOKI, T., Upper extremity interaction with a deploying side airbag: a characterization of elbow joint loading. *Accident Analysis and Prevention*. 35(3): 417-425, 2003b.

DUMA, S.M., KEMPER, A.R., STITZEL, J.D., MCNALLY, C., KENNEDY, E.A., AND MATSUOKA, F., Rib fracture timing in dynamic belt tests with human cadavers. Clin. Anat. 24, 327-38, 2011.

EJIMA, S., ONO, K., HOLCOMBE, S., KANEOKA, K., FUKUSHIMA, M., Prediction of the physical motion of the human body based on muscle activity during pre-impact bracing. Proceedings of the IRCOBI Conference. 163-175, 2008.

EPPINGER, RH. Prediction of thoracic injury using measurable experimental parameters. Proceedings of the 6th International Technical Conference on the Enhanced Safety of Vehicles. pp. 770-779, 1976. National Highway Traffic Safety Administration; Washington, DC.

EPPINGER, R., On the development of a deformation measurement system and its application toward developing mechanically based injury indices. Proceedings 33rd Stapp Car Crash Conference. SAE 892426, 21-28., 1989.

FORMAN, J., LESSLEY, D., SHAW, C.G., EVANS, J., KENT, R., ROUHANA, S.W., AND PRASAD, P., Thoracic response of belted PMHS, the Hybrid III, and the THOR-NT mid-sized male surrogates in low speed, frontal crashes. Stapp Car Crash Journal, 50, 191-215, 2006.

GABLER, H, DIGGES, K., FILDES, B., AND SPARKS, L., Side impact risk for belted far side passenger vehicle occupants. Society of Automotive Engineers, Warrendale, PA, 2005.

GAYZIK, F.S., MARTIN, R.S., GABLER, H.C., HOTH, J.J., DUMA, S.M., MEREDITH, J.W., AND STITZEL, J.D., Characterization of crash-induced thoracic loading resulting in pulmonary contusion. J Trauma, 66, 840-9, 2009.

HENDLER, E., O'ROURKE, J., SCHULMAN, M., KATZEFF, M., DOMZALSKI, L., AND RODGERS, S., Effect of head and body position and muscular tensing on response to impact. SAE Technical Paper Series; SAE 741184, 1974.

JERNIGAN, M.V., RATH, A.L., AND DUMA, S.M., Severe upper extremity injuries in frontal automobile crashes: the effects of depowered airbags. Am J Emerg Med. 23, 99-105, 2005.

KALLIERIS, D., RIZZETTI, A., MATTERN, R., MORGAN, R., EPPINGER, R., AND KEENAN, L., On the synergism of the driver air bag and 3-point belt in frontal collisions. Proceedings 39th Stapp Car Crash Conference. SAE 952700, 389-402, 1995.

KENNEDY, E.A., HURST, W.J., STITZEL, J.D., CORMIER, J.M., HANSEN, G.A., SMITH, E.P., AND DUMA, S.M., Lateral and posterior dynamic bending of the mid-shaft femur: fracture risk curves for the adult population. Stapp Car Crash J. 48, 27-51, 2004.

KEMPER, A.R., MCNALLY, C., KENNEDY, E.A., MANOOGIAN, S.J., AND DUMA, S.M., The influence of arm position on thoracic response in side impacts. Stapp Car Crash J. 52, 379-420, 2008.

KEMPER, A.R., STITZEL, J.D., MCNALLY, C., GABLER, H.C., AND DUMA, S.M., Biomechanical response of the human clavicle: the effects of loading direction on bending properties. J. Appl. Biomech., 25, 165-74, 2009.

KUPPA, S.M., AND EPPINGER, R.H. Development of an improved thoracic injury criterion. Proceedings of the 42nd Stapp Car Crash Conference, pp. 139-154, 1998. Society of Automotive Engineers; Warrendale, PA.

KUPPA, S., EPPINGER, R., MCKOY, F., NGUYEN, T., PINTAR, F., AND YOGANANDAN N. Development of side impact thoracic injury criteria and their application to the modified ES-2 dummy with rib extensions. *Stapp Car Crash Journal,* 47: 189-210, 2003.

MORGAN, R., MARCUS, J., AND EPPINGER, R. Side Impact – the Biofidelity of NHTSA's Proposed ATD and Efficacy of TTI. Proceedings of the 13th Stapp Car Crash Conference, pp. 27-40, 1986. Society of Automotive Engineers; Warrendale, PA.

MORGAN, R.M., EPPINGER, R.H., HAFFNER, M.P., KALLIERIS, D., MILTNER, E., MATTERN, R., AND KLOPP, G.S. Thoracic trauma assessment formulations for restrained drivers in simulated frontal impacts. *Stapp Car Crash Journal, 38*: 15-34, 1994.

NHTSA Traffic Safety Facts 2008. Washington, DC, National Highway Traffic Safety Administration.

PINTAR, F., YOGANANDAN, N., HINES, M., MALTESE, M., MCFADDEN, J., SAUL, R., EPPINGER, R., KHAEWPONG, N., AND KLEINBERGER, M. Chestband analysis of human tolerance to side impact. Proceedings of the 41st Stapp Car Crash Conference. pp. 63-74, 1997. Society of Automotive Engineers; Warrendale, PA.

SAE J211 "Instrumentation for Impact Test," SAE J211/1 MAR 1995, 1995 SAE Handbook Volume 4 - On-Highway Vehicles & Off-Highway Machinery, Society of Automotive Engineers, Warrendale, PA. 1995.

SAMAHA, R., AND ELLIOTT, D., NHTSA Side Impact Research: Motivation for Upgraded Test Procedures, Eighteenth International Technical Conference on the Enhanced Safety of Vehicles, Paper No. 03-492, 2003.

SCHNEIDER, L. W.; Development of anthropometrically based design specifications for an advanced adult anthropomorphic dummy family; NHTSA; 1, 1983.

SHAW, J.M., HERRIOTT, R.G., MCFADDEN, J.D., DONNELLY, B.R., AND BOLTE, J.H., Oblique and lateral impact response of the PMHS thorax. Stapp Car Crash Journal. 50, 146-167, 2006.

SUGIYAMA, T., KIMPARA, H., IWAMOTO, M., YAMADA, D., Effects of muscle tense on impact responses of lower extremity. Proceedings of the IRCOBI Conference. Maastricht, Netherlands, 127-139, 2007.

VIANO D. Biomechanical Responses and Injuries in Blunt Lateral Impact. Proceedings of the 33rd Stapp Car Crash Conference, pp. 113-142, 1989. Society of Automotive Engineers; Warrendale, PA.

YOGANANDAN, N., SKRADE, D., PINTAR, F., REINARTZ, J., AND SANCES, A., Thoracic deformation contours in a frontal impact, Proceedings of the 35th Stapp Car Crash Conference San Diego. SAE 912891, 47–63, 1991.